PHYSICAL REVIEW D **76,** 103516 (2007)

Bulk viscous cosmology

R. Colistete, Jr.,[1,*] J. C. Fabris,[1,†] J. Tossa,[2,‡] and W. Zimdahl[1,§]

[1]*Universidade Federal do Espírito Santo, Departamento de Física, Av. Fernando Ferrari, 514, Campus de Goiabeiras, CEP 29075-910, Vitória, Espírito Santo, Brazil*

[2]*Institut de Mathématiques et de Sciences Physiques—IMSP, Université d'Abomey-Calavi, BP613, Porto Novo, Benin*

(Received 27 June 2007; published 8 November 2007)

We propose a scenario in which the dark components of the Universe are manifestations of a single bulk viscous fluid. Using dynamical system methods, a qualitative study of the homogeneous, isotropic background scenario is performed in order to determine the phase space of all possible solutions. The specific model which we investigate shares similarities with a generalized Chaplygin gas in the background but is characterized by nonadiabatic pressure perturbations. This model is tested against supernova type Ia and matter power spectrum data. Different from other unified descriptions of dark matter and dark energy, the matter power spectrum is well behaved, i.e., there are no instabilities or oscillations on small perturbation scales. The model is competitive in comparison with the currently most popular proposals for the description of the cosmological dark sector.

DOI: 10.1103/PhysRevD.76.103516 PACS numbers: 98.80.Jk, 95.35.+d, 98.80.Es

I. INTRODUCTION

The crossing of observational data from high redshift supernovae of type Ia (SNe Ia) [1–4], cosmic microwave background (CMB) radiation [5], matter power spectra [6], x rays from clusters of galaxies [7,8], and weak gravitational lensing [9] strongly suggests that the present Universe is dynamically dominated by a dark sector which is responsible for about 96% of its total energy content. It is usually assumed that this dark sector has two different components: (i) dark matter, which is supposed to consist of weakly interacting massive particles (WIMPS) with zero effective pressure and (ii) dark energy, a mysterious entity which is equipped with a negative pressure. Dark matter candidates include axions (a particle present in the multiplet of grand unified theories) and neutralinos (light particles present in broken supersymmetric models), but none of these particles could be detected until now. The most natural dark energy candidate is a cosmological constant which arises as the result of a combination of quantum field theory and general relativity. However, its theoretical value is between 60–120 orders of magnitude greater than the observed value for the dark energy. An alternative to the cosmological constant is a self-interacting scalar field, known as quintessence. For a brief but enlightening review of these and other proposals, see [10] and references therein.

There exists another route of investigations in which dark matter and dark energy are described within a one-component model. According to this idea, dark matter and dark energy are just "different faces" of a single, exotic fluid. To the best of our knowledge, the first proposal along this line was the Chaplygin gas in its original and modified forms [11–13]. However, this unified description of dark energy and dark matter, in spite of many attractive features, seemed to suffer from a major drawback: it predicted strong small scale oscillations or instabilities in the matter power spectrum, in complete disagreement with the observational data [14]. (On the other hand, the observed matter power spectrum corresponds to the baryonic matter distribution which does not exhibit strong oscillations [15], so that this point is still controversial.) The apparently unrealistic predictions of the unified Chaplygin gas type models are the result of an adiabatic perturbation analysis. It has been suggested that nonadiabatic perturbations may alleviate or even avoid this problem [16–18].

This paper explores to what extent a viscous fluid can provide a unified description of the dark sector of the cosmic medium. The general influence of shear and bulk viscosity on the character of cosmological evolution has been studied, e.g. in [19], in the context of Bianchi type I models. Under the conditions of spatial homogeneity and isotropy, a scalar bulk viscous pressure is the only admissible dissipative phenomenon. The cosmological relevance of bulk viscous media has been investigated in some detail for an inflationary phase in the early universe (see [20–24] and references therein). However, as was argued in [16,25], an effective bulk viscous pressure can also play the role of an agent that drives the present acceleration of the Universe. (Notice that the possibility of a viscosity dominated late epoch of the Universe with accelerated expansion was already mentioned in [26]). For a homogeneous and isotropic universe, the ΛCDM model and the (generalized) Chaplygin gas models can be reproduced as special cases of this imperfect fluid description [16]. Moreover, in a gas dynamical model the existence of an effective bulk pressure can be traced back to a nonstandard self-interacting force on the particles of the gas. While these investigations were performed for the homogeneous and

*rcolistete@terra.com.br
†fabris@pq.cnpq.br
‡joel.tossa@imsp-uac.org
§zimdahl@thp.uni-koeln.de

isotropic background dynamics (a study of the background dynamics which is similar to the setup of the present paper was recently performed in [27]), a first perturbation theoretical analysis for a unifying viscous fluid description of the dark sector was performed in [28].

The bulk viscous pressure $p_{\rm visc}$ will be described by Eckart's expression [29] $p_{\rm visc} = -\xi u^{\mu}_{;\mu}$, where the (nonnegative) quantity ξ is the (generally not constant) bulk viscosity coefficient and $u^{\mu}_{;\mu}$ is the fluid expansion scalar which in the homogeneous and isotropic background reduces to $3H$, where $H = \frac{\dot{a}}{a}$ is the Hubble parameter and a is the scale factor of the Robertson-Walker metric. By this assumption we ignore all the problems inherent in Eckart's approach which have been discussed and resolved within the Israel-Stewart theory [30,31] (see also [21–24] and references therein). We expect that for the applications we have in mind here, the differences are of minor importance.

It is obvious that the bulk viscosity contributes with a negative term to the total pressure and hence a dissipative fluid seems to be a potential dark energy candidate. However, a cautionary remark is necessary here. In traditional nonequilibrium thermodynamics the viscous pressure represents a (small) correction to the (positive) equilibrium pressure. This is true both for the Eckart and for the Israel-Stewart theories. Here we shall admit the viscous pressure to be the dominating part of the pressure. This is clearly beyond the established range of validity of conventional nonequilibrium thermodynamics. As already mentioned, nonstandard interactions are required to support such type of approach [16,25]. Of course, this reflects the circumstance that dark energy is anything but a "standard" fluid. (We mention that viscosity has also been suggested to have its origin in string landscape [32]). To successfully describe the transition to a phase of accelerated expansion, preceded by a phase of decelerated expansion in which structures can form, it is necessary that the viscous pressure is negligible at high redshifts but becomes dominant later on.

In Ref. [28] a one-component bulk viscous model (BV model) of the cosmic medium was investigated in which baryons were not taken into account. As far as the SNe Ia data are concerned, the results of this model were similar to those obtained for a generalized Chaplygin gas (GCG) model. But while GCG models predict small scale instabilities and oscillations at the perturbative level, the corresponding matter power spectrum of the BV model turned out to be well behaved. Of course, the results of a model that does not include baryons cannot be seen as conclusive; after all, the observed power spectrum describes the distribution of baryonic matter. In the present paper, we perform an advanced analysis which properly includes a separately conserved baryon component. Thus we establish a more realistic viscous fluid scenario of the cosmic substratum.

For the quantitative calculations we will use a constant coefficient of bulk viscosity. A qualitative analysis with the help of dynamical system methods is applied to visualize the space of more general cosmological background scenarios. The corresponding phase space reveals interesting new features compared with those generally found in similar models (see, for example, [33] and references therein). In the present approach there is an entire singular axis. Solutions of the desired type are generated, i.e., solutions for which an initial subluminal expansion is followed by superluminal expansion. These solutions are characterized by a bulk viscosity coefficient with a power law dependence on the energy density, $\xi = \xi_0 \rho^{\nu}$, where $\xi_0 = \text{const}$ and $\nu < 1/2$.

We test the results of our model both against SNe Ia data and the observed matter power spectrum. Both the results for type Ia supernovae and for the matter power spectrum show that the BV model is competitive with the ΛCDM model as well as with quintessence and different Chaplygin gas type models. In particular, our minimum χ^2 value for the SNe Ia data is similar to the χ^2 values of those models. Furthermore, the matter power spectrum represents a good fit to the corresponding observational data. We argue that the absence of oscillations and instabilities is a consequence of the fact that the pressure perturbations in our model are intrinsically nonadiabatic.

The paper is organized as follows. In Sec. II we define our model and specify the homogeneous and isotropic background dynamics. Section III performs a qualitative analysis using dynamical system methods. In Sec. IV, the SNe Ia data are used to restrict the values of the physically relevant free parameters. In Sec. V the matter power spectrum is determined and compared with large scale structure observations. In Sec. VI we present our conclusions.

II. BACKGROUND RELATIONS

A bulk viscous fluid is characterized by an energy density ρ and a pressure p which has a conventional component $p_{\beta} = \beta\rho$ and a bulk viscosity component $p_{\rm visc} = -\xi(\rho) u^{\mu}_{;\mu}$, such that

$$p = \beta\rho - \xi(\rho) u^{\mu}_{;\mu}. \quad (1)$$

On thermodynamical grounds the bulk viscosity coefficient $\xi(\rho)$ is positive, assuring that the viscosity pushes the effective pressure towards negative values. In fact, the expression (1) is the original proposition for a relativistic dissipative process [29]. As already mentioned, it follows from the more general Israel-Stewart theory [30,31] in the limit of a vanishing relaxation time. We shall assume this approximation to be valid throughout the paper.

Let us consider the cosmic medium to consist of a viscous fluid of the type (1), which is supposed to characterize the dark sector, and of a pressureless fluid that describes the baryon component. Hence, the relevant set of equations is

$$R_{\mu\nu} - \frac{1}{2}g_{\mu\nu}R = 8\pi G\{T^{v}_{\mu\nu} + T^{b}_{\mu\nu}\}, \tag{2}$$

$$T_v^{\mu\nu}{}_{;\mu} = 0, \qquad T_v^{\mu\nu} = (\rho_v + p_v)u^\mu u^\nu - p_v g^{\mu\nu}, \tag{3}$$

$$p = p_v = \beta\rho_v - \xi(\rho_v)u^\mu{}_{;\mu}, \tag{4}$$

$$T_b^{\mu\nu}{}_{;\mu} = 0, \qquad T_b^{\mu\nu} = \rho_m u^\mu u^\nu. \tag{5}$$

The (super)subscripts v and b indicate the viscous and the (baryonic) matter components, respectively. Since the matter is pressureless, the total pressure p of the cosmic medium coincides with the pressure p_v of the viscous fluid. For the homogeneous and isotropic background dynamics we shall restrict ourselves to the flat Friedmann-Lemaître-Robertson-Walker (FRLW) metric,

$$ds^2 = dt^2 - a^2(t)(dx^2 + dy^2 + dz^2), \tag{6}$$

favored by the CMB anisotropy spectrum [5]. The dynamic equations then are:

$$\left(\frac{\dot a}{a}\right)^2 = \frac{8\pi G}{3}(\rho_b + \rho_v), \tag{7}$$

$$2\frac{\ddot a}{a} + \frac{\dot a^2}{a^2} = -8\pi G p_v \tag{8}$$

$$\dot\rho_v + 3\frac{\dot a}{a}(\rho_v + p_v) = 0, \tag{9}$$

$$\dot\rho_b + 3\frac{\dot a}{a}\rho_b = 0, \tag{10}$$

$$p_v = \beta\rho_v - 3\frac{\dot a}{a}\xi_0\rho_v^\nu, \tag{11}$$

where the bulk viscosity coefficient was assumed to have a power law dependence on the energy density ρ_v according to $\xi(\rho_v) = \xi_0\rho_v^\nu$ with $\xi_0 = $ const. The dot denotes differentiation with respect to the cosmic time. Of course, not all these equations are independent. Equation (10) is decoupled and leads to

$$\rho_b = \frac{\rho_{b0}}{a^3}. \tag{12}$$

Here and in the following, quantities with a subscript 0 refer to the present epoch and we have used $a_0 = 1$. From now on we will set $\beta = 0$, thus assuming the dissipative pressure to be the dominating contribution.

With a change of variables,

$$\dot\rho_v = \frac{d\rho_v}{dt} = \frac{d\rho_v}{da}\frac{da}{dt} = \rho_v'\dot a, \tag{13}$$

where the prime means derivative with respect to the scale factor a, and using relation (7), the conservation equation for the viscous component becomes

$$\rho_v' + \frac{3}{a}\left(\rho_v - 3\frac{\dot a}{a}\xi_0\rho_v^\nu\right) = 0. \tag{14}$$

This equation can be recast in an integral form:

$$\int\frac{d\varepsilon}{\varepsilon^\nu(\varepsilon+1)} = \frac{2k}{3(1-2\nu)}a^{(3/2)(1-2\nu)}, \qquad \nu \neq \frac{1}{2}; \tag{15}$$

$$\int\frac{d\varepsilon}{\varepsilon+1} = k\ln a, \qquad \nu = \frac{1}{2}; \tag{16}$$

$$\varepsilon = \frac{\rho_v}{\rho_b}, \qquad k = 9\sqrt{\frac{8\pi G}{3}}\xi_0\rho_{b0}^{\nu-(1/2)}. \tag{17}$$

We will be mainly interested in the case $\nu \neq \frac{1}{2}$.

There is a simple, direct relation between ρ_v and the scale factor a for $\nu = 0$. In this particular case, we find,

$$\rho_v = \rho_b\left\{\left[B + \frac{k}{3}a^{(3/2)}\right]^2 - 1\right\}, \qquad (\nu = 0), \tag{18}$$

where B is an integration constant. It can easily be verified that $\rho_v \to a^{-3}$ when $a \to 0$ (pressureless matter) and $\rho_v \to$ cte (cosmological constant) when $a \to \infty$. It is expedient to notice that for $\nu = 0$ the total energy density $\rho = \rho_v + \rho_b$ coincides with the energy density of a specific GCG [11–13]. Generally, a GCG is characterized by an equation of state ($E = $ const > 0)

$$p_{\rm GCG} = -\frac{E}{\rho_{\rm GCG}^\alpha}, \tag{19}$$

which corresponds to an energy density

$$\rho_{\rm GCG} = \left[E + \frac{F}{a^{3(1+\alpha)}}\right]^{1/(1+\alpha)}, \tag{20}$$

where F is another (non-negative) constant. With the identifications $E = \frac{k}{3}\rho_{b0}^{1/2}$ and $F = B\rho_{b0}^{1/2}$ it becomes obvious that for $\alpha = -1/2$ the energy densities $\rho = \rho_v + \rho_b$ from (18) and $\rho_{\rm GCG}$ in (20) coincide. The analogy between dissipative and GCG models was also pointed out in [27].

The structure of the total energy density $\rho = \rho_v + \rho_b$ allows us to perform a decomposition of the viscous-baryon system into three noninteracting components plus the baryonic fluid:

$$\rho = \rho_1 + \rho_2 + \rho_3 + \rho_b, \tag{21}$$

with

$$\rho_1 = E^2, \qquad \rho_2 = 2\frac{EF}{a^{3/2}},$$
$$\rho_3 = \frac{F^2 - \rho_{b0}}{a^3}, \qquad \rho_b = \frac{\rho_{b0}}{a^3}, \tag{22}$$

and

$$E = \frac{k}{3}\sqrt{\rho_{b0}}, \qquad F = \sqrt{\rho_{b0}}B. \tag{23}$$

The individual equations of state of the different components are:

$$p_1 = -\rho_1, \qquad p_2 = -\tfrac{1}{2}\rho_2, \qquad p_3 = 0, \qquad p_b = 0. \tag{24}$$

Consequently, our system is equivalent to a mixture of two dark energy type fluids, one dark matter fluid and the baryon component. While the BV model is a unified description of dark matter/energy, the option of a decomposition may be useful in comparing the scenario with some observational data. The x-ray measurement of galactic clusters [34] is an example which requires a separation of a matter component of the cosmic medium. For a Chaplygin gas, different decompositions have been proposed in the literature [18,35]. Moreover, the decomposition (21) with (22)–(24) reveals that the background dynamics of our model differs from that of the ΛCDM model (including a baryon component) by the existence of the second dark energy component with energy density ρ_2.

The relevant cosmological quantities are the present density parameters Ω_{v0} and Ω_{b0} which represent the fractions of the viscous fluid and of the pressureless matter, respectively, with respect to the total density (remember that we restrict ourselves to the flat case), the Hubble parameter today H_0, the present value of the deceleration parameter q_0, and the age of the universe t_0. The apparently new parameter of the present model, the viscosity coefficient, can be expressed in terms of the other quantities. In fact, the relation (18) can be rewritten in a more convenient way. Using Friedmann's equation today, we have

$$H_0^2 = \frac{8\pi G}{3}(\rho_{b0} + \rho_{v0}) \Rightarrow \Omega_{v0} + \Omega_{b0} = 1, \tag{25}$$

$$\Omega_{b0} = \frac{8\pi G}{3H_0^2}\rho_{b0}, \qquad \Omega_{v0} = \frac{8\pi G}{3H_0^2}\rho_{v0}. \tag{26}$$

Combining (18) with (25) and (26) we obtain the relation

$$B + \frac{k}{3} = \frac{1}{\sqrt{\Omega_{b0}}}. \tag{27}$$

Now, if we use Eq. (8) with $p = p_v = -3\xi_0 \frac{\dot{a}}{a}$ and the definition of the deceleration parameter $q_0 = -\frac{\ddot{a}a}{\dot{a}^2}$, we find

$$-2q_0 + 1 = \frac{24\pi G\xi_0}{H_0}. \tag{28}$$

From the definition of k in Eq. (17) we have

$$k = \frac{24\pi G\xi_0}{H_0}\frac{1}{\sqrt{\Omega_{b0}}}. \tag{29}$$

Using Eq. (8), evaluated today, it follows that

$$k = \frac{1 - 2q_0}{\sqrt{\Omega_{b0}}}, \tag{30}$$

which leads to

$$B = \frac{2}{3}\frac{1 + q_0}{\sqrt{\Omega_{b0}}}. \tag{31}$$

Hence, the viscous fluid energy density becomes

$$\rho_v = \rho_b\{f^2(a) - 1\}, \qquad f(a) = \frac{1}{3\sqrt{\Omega_{b0}}}[2(1 + q_0) + (1 - 2q_0)a^{3/2}]. \tag{32}$$

All these relations will be useful for defining the observables that will be constrained later on by the SNe Ia and matter power spectrum data.

III. A DYNAMICAL SYSTEM ANALYSIS

The relations of the previous section that will be used to compare the theoretical predictions of our model with observational data are valid under the restriction $\nu = 0$. It is important to have an idea of how serious this restriction is. If the case $\nu = 0$ is very particular, our results will not be conclusive. Therefore it is desirable to have at least a qualitative analysis of the general case (7)–(11) which, because of its complexity, cannot be solved analytically. Such an analysis could reveal whether or not the case $\nu = 0$ is, in a sense, typical. To this purpose we shall use dynamical system techniques for a system of nonlinear differential equation [36].

The system of equations (7)–(11) can be recast in a more convenient form by using geometric unities $8\pi G = 1$ and fixing the scale so that $\xi_0 = 1$. Defining $x = \frac{\dot{a}}{a}$ and $y = \rho_v$, the following system of equations is obtained:

$$\dot{x} = -\tfrac{3}{2}x(x - y^\nu) = P(x, y), \tag{33}$$

$$\dot{y} = -3xy(1 - 3xy^{\nu-1}) = Q(x, y). \tag{34}$$

Since the density $\rho_b = 3x^2 - y$ of the baryonic matter must be non-negative, the solutions that have physical meaning are those which satisfy $y \le 3x^2$.

In a first step we have to identify the critical points (x_0, y_0) for which $P(x_0, y_0) = Q(x_0, y_0) = 0$. These points are either attractors or repellers or saddle points. The nature of a critical point is determined by the eigenvalues of the matrix

$$\begin{pmatrix} P_x(x_0, y_0) & P_y(x_0, y_0) \\ Q_x(x_0, y_0) & Q_y(x_0, y_0) \end{pmatrix},$$

where $P_{x^i} = \frac{\partial P}{\partial x^i}$, $x^i = x, y$ and $Q_{x^i} = \frac{\partial Q}{\partial x^i}$. In general, there are two eigenvalues $\lambda_{1,2}$ for the characteristic equation of this matrix. If both eigenvalues are positive, than the critical point is a repeller; if both are negative, the critical point is an attractor; if one is positive and the other one is negative, then the critical point is a saddle. With the help of a suitable transformation [36], the critical points at infinity can be studied. A projection onto the Poincaré sphere [36]

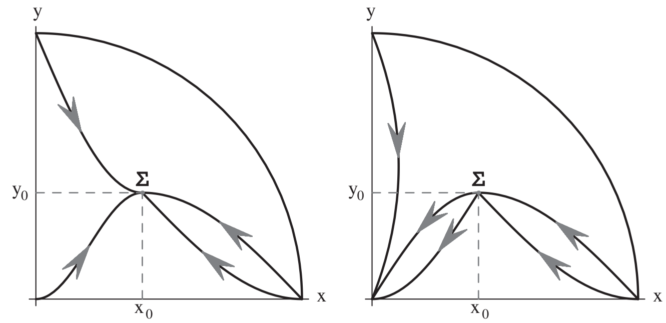

FIG. 1. Phase diagrams for $\nu < 1/2$ (upper panel) and for $1/2 < \nu < 3/2$ (lower panel). For $\nu > 3/2$ the directions of the arrows in the lower panel have to be reversed.

will then allow us to represent the entire phase space in a finite region in the x-y plane.

It turns out that the entire Oy axis is a stationary solution for the system, representing a static space-time. A singular point, denoted by Σ, is $(x_0, y_0) = (3^{\nu/(1-2\nu)}, 3^{1/(1-2\nu)})$ where $\nu \neq \frac{1}{2}$. The characteristic equation for this critical point is given by $\lambda^2 + \alpha_0(\frac{3}{2} - \nu)\lambda + \alpha_0^2(\frac{1}{2} - \nu) = 0$ where $\alpha_0 = 3^{(1-\nu)/(1-2\nu)}$. The eigenvalues are $\lambda_1 = (\nu - \frac{1}{2})\alpha_0$ and $\lambda_2 = -\alpha_0$. The phase diagram depends on the value of the parameter ν. If $\nu < 1/2$, the critical point Σ is an attractor: all solutions converge to it. This point represents the de Sitter phase. Hence, all solutions approach a de Sitter phase asymptotically.

If $1/2 < \nu < 3/2$, the point Σ becomes a saddle point and all solutions approach a Minkowski space-time in the origin. If $\nu > 3/2$, Σ is still a saddle point, but the directions of the curves change: all solutions leave the Minkowski space-time. These different behaviors are shown in Fig. 1. For the point Σ we have $3x_0^2 = y_0^2$, which corresponds to a vanishing baryon density. (Recall that the range $y > 3x^2$ is unphysical.) The deceleration parameter q can be written as $q = -1 - \frac{\dot{H}}{H^2}$, equivalent to $q = -1 - \frac{\dot{x}}{x^2}$. Combination with Eq. (33) shows that there is accelerated expansion $q < 0$ for $x < 3y^\nu$. The special case $\nu = 0$ has $(x_0, y_0) = (1, 3)$ and accelerated expansion for $x < 3$. This solution is of the type of the curves that approach the point Σ from right below in the left panel of Fig. 1. Notice that there is a projection effect due to the circumstance that infinity is mapped onto one single point on the x axis. The curve that points from the origin towards Σ in the left part of Fig. 1 corresponds to a phantom scenario with $\rho_b = 0$ which separates the physical and unphysical regions. We are not interested here in this type of models.

IV. CONSTRAINING THE MODEL USING SNE IA DATA

The type Ia supernovae allow us to obtain information about the Universe at high redshifts. Today, observers have detected about 300 of these objects with redshifts up to almost 2. In what follows, we will use the more restricted sample of 182 SNe Ia of the Gold06 data set which consists of objects for which the observational data are of very high quality [37]. The relevant quantity for our analysis is the moduli distance μ, which is obtained from the luminosity distance D_L by the relation

$$\mu = 5\log\left(\frac{D_L}{\mathrm{Mpc}}\right) + 25. \tag{35}$$

The computation of the luminosity distance follows the standard procedure [1,38]. First, we recall its definition [39,40],

$$D_L = \frac{r}{a} = (1+z)r, \tag{36}$$

where r is the comoving coordinate of the source and z is the redshift, $z = -1 + \frac{1}{a}$. The coordinate r can be obtained by considering the propagation of light $ds^2 = 0$. This implies

$$ds^2 = c^2dt^2 - a^2dr^2 = 0 \Rightarrow r = -c\int_1^a \frac{da}{a\dot{a}}. \tag{37}$$

From Friedmann's equation one obtains

$$\dot{a} = \sqrt{\frac{\Omega_{m0}}{a}}H_0 f(a). \tag{38}$$

In terms of the redshift z, the luminosity distance may be expressed as

$$D_L = 3(1+z)\frac{c}{H_0}\int_0^z \frac{dz'}{2(1+q_0)(1+z')^{3/2} + (1-2q_0)}, \tag{39}$$

or, using B and Ω_{m0},

$$D_L = (1+z)\frac{c}{H_0}\int_0^z \frac{dz'}{1 + \sqrt{\Omega_{m0}}B((z'+1)^{3/2} - 1)}. \tag{40}$$

In order to compare the theoretical results with the observational data, the first step is to compute the quality of the fitting through the least square fitting quantity χ^2. We adopt the HST (Hubble Space Telescope) prior [41] for H_0, as well as the cosmic nucleosynthesis prior for the baryonic density parameter $\Omega_{b0}h^2$ (where h is H_0 divided by 100 km/s/Mpc), which leads to

$$\chi^2 = \sum_i \frac{(\mu_{0,i}^o - \mu_{0,i}^t)^2}{\sigma_{\mu_0,i}^2} + \frac{(h-0.72)^2}{0.08^2} + \frac{(\Omega_{b0}h^2 - 0.0214)^2}{0.0020^2}. \tag{41}$$

The quantities $\mu_{0,i}^o$ are the distance moduli, observationally measured for each supernova of the 182 Gold06 SNe Ia data set [37] and the $\mu_{0,i}^t$ are the corresponding theoretical values. The $\sigma_{\mu_0,i}^2$ represent the measurement errors and include the dispersion in the distance moduli, resulting from the galaxy redshift dispersion which is due to the peculiar velocities of the objects (cf. [3,37]).

The smaller the χ^2, the better the agreement between the theoretical model and the observational data. Table I shows that the χ^2 value for the BV model is competitive with the GCG model (cf. Eq. (20)), the traditional Chaplygin gas model (cf. Eq. (20) with $\alpha = 1$) and the ΛCDM model. Compared with the ΛCDM and the (generalized) Chaplygin gas models, the age of the Universe is greater for the bulk viscous model and its deceleration parameter is less negative, i.e., the Universe is less accelerated.

Using Bayesian statistics, a probability distribution can be constructed from the χ^2 parameter [38]. In the present case, there are three free parameters: the Hubble parameter today H_0, the pressureless baryonic density parameter Ω_{b0}, and the auxiliary quantity B which is connected to the present value of the deceleration parameter (cf. (31)). Marginalization over one or two of these parameters will lead to corresponding two- or one-dimensional representations. The details of the Bayesian statistics and computational analysis, relying on BETOCS (BayEsian Tools for Observational Cosmology using SNe Ia), are given in Ref. [38].

The main feature of the parameter estimation for the viscous fluid model is the Gaussian-like distribution around the preferred value.

This can easily be seen both in Table II (almost symmetric error bars) and in the two and one-dimensional diagrams of Figs. 2 and 3. In Fig. 2 we show the two-dimensional probability distribution for the parameters B, Ω_{b0}, and H_0 at one, two, and three sigma, corresponding, respectively, to 68%, 95%, and 99% confidence levels. The corresponding one-dimensional probability distributions are shown in Fig. 3. The main features of the model are: the age of the Universe is considerably larger than for the ΛCDM and GCG models, around $t_0 \sim 16$ Gy, with a small dispersion; the baryon density is around 0.05, a little larger than predicted by nucleosynthesis, but there is a marginal

TABLE I. The best-fitting parameters, i.e., when χ^2 is minimum, for the BV model, the GCG model, the traditional Chaplygin gas model ($\alpha = 1$), and the ΛCDM model ($\alpha = 0$) for a flat universe ($\Omega_{k0} = 0$). H_0 is given in km/Mpc.s, $\bar{E} \equiv \frac{E}{E+F}$ in units of c^2 (c—speed of light) and t_0 in Gy.

	Bulk viscosity	Generalized Chaplygin gas	Traditional Chaplygin gas	ΛCDM
χ^2	162.71	157.52	157.88	160.07
B	1.81	—	—	—
α	—	1.90	1	0
$\bar{E}$	—	0.897	0.825	1
Ω_{b0}	0.0550	0.0523	0.0530	0.054
Ω_{dm0}	—	—	—	0.284
H_0	62.38	63.97	63.56	62.8695
t_0	15.92	13.83	14.09	14.83
q_0	−0.364	−0.775	−0.672	−0.493

TABLE II. The estimated parameters for the BV model, the GCG model, the traditional Chaplygin gas model, and the ΛCDM model for a flat universe ($\Omega_{k0} = 0$). We use the Bayesian analysis to obtain the peak of the one-dimensional marginal probability and the 2σ confidence region for each parameter. H_0 is given in km/s/Mpc, $\bar{E} \equiv \frac{E}{E+F}$ in units of c^2 (c—speed of light) and t_0 in Gy.

	Bulk viscosity	Generalized Chaplygin gas	Traditional Chaplygin gas	ΛCDM
B	$1.81^{+0.38}_{-0.34}$	—	—	—
α	—	$1.25^{+4.24}_{-1.78}$	1	0
$\bar{E}$	—	$0.943^{+0.056}_{-0.265}$	$0.825^{+0.057}_{-0.074}$	1
Ω_{b0}	$0.055^{+0.011}_{-0.011}$	$0.053^{+0.011}_{-0.010}$	$0.053^{+0.011}_{-0.010}$	$0.054^{+0.011}_{-0.010}$
Ω_{dm0}	—	—	—	$0.284^{+0.082}_{-0.072}$
H_0	$62.34^{+1.75}_{-1.72}$	$63.74^{+1.93}_{-2.07}$	$63.45^{+1.76}_{-1.79}$	$62.80^{+1.76}_{-1.75}$
t_0	$15.85^{+1.08}_{-0.91}$	$13.72^{+1.21}_{-0.62}$	$14.04^{+0.57}_{-0.05}$	$14.80^{+0.73}_{-0.62}$
q_0	$-0.357^{+0.130}_{-0.123}$	$-0.816^{+0.362}_{-0.133}$	$-0.671^{+0.109}_{-0.087}$	$-0.502^{+0.136}_{-0.103}$
$p(q_0 < 0)$	6.22σ	100%	100%	100%

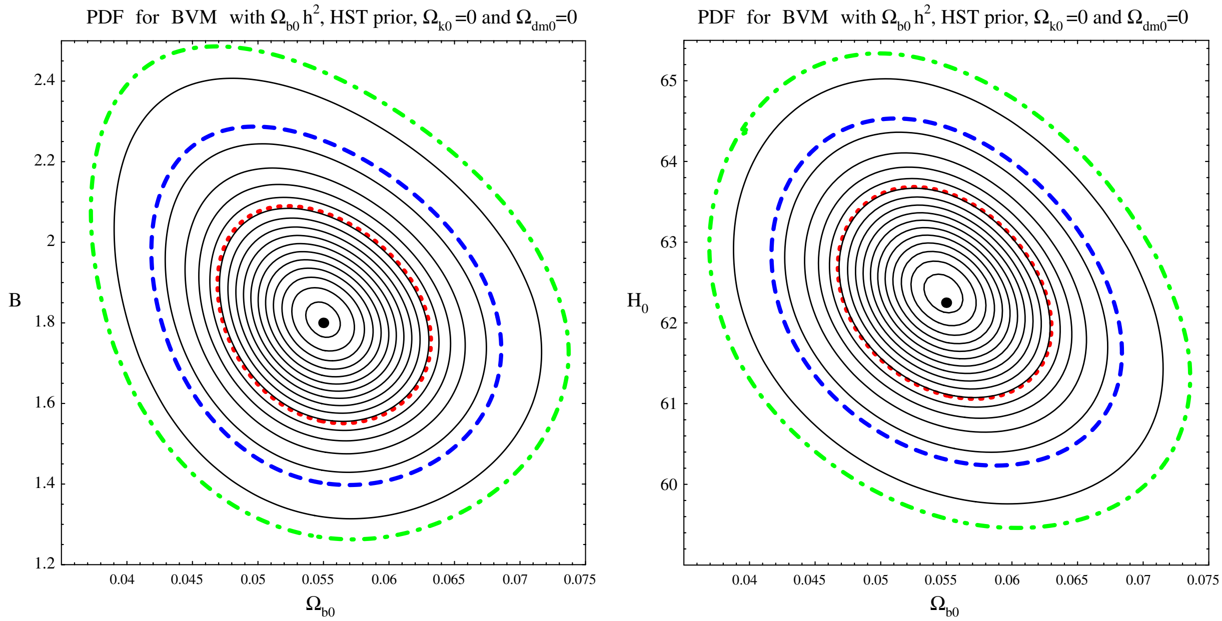

FIG. 2 (color online). The two-dimensional plots of the probability density function (PDF) as a function for the parameter B, the baryon density, and the Hubble constant. The joint PDF peak is shown by the large dot, the confidence regions of 1σ (68, 27%) by the red dotted line, the 2σ (95, 45%) in the blue dashed line, and the 3σ (99, 73%) in the green dashed-dotted line.

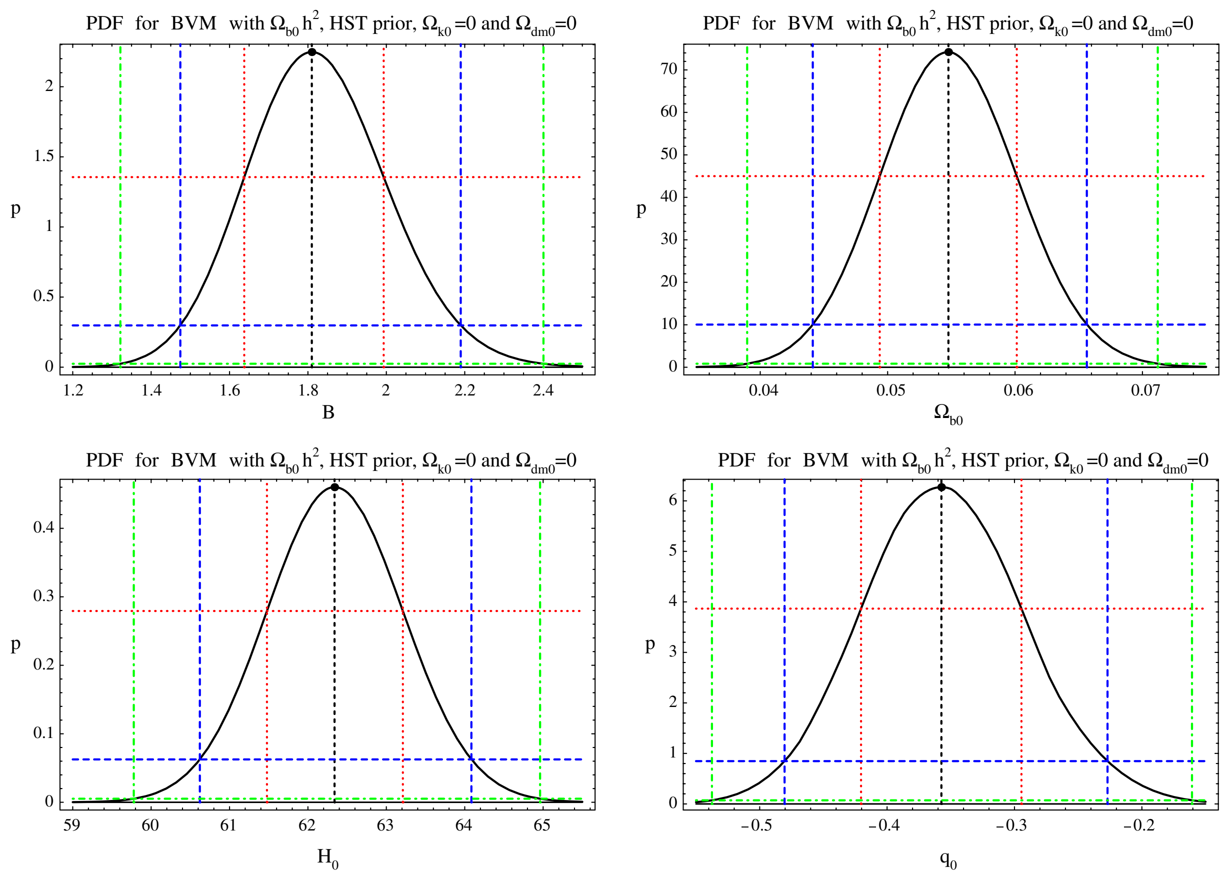

FIG. 3 (color online). The one-dimensional plots of the PDF as a function for the parameter B, the baryonic density, the Hubble constant, and the deceleration parameter. The joint PDF peak is shown by the large dot, the confidence regions of 1σ (68, 27%) by the red dotted line, the 2σ (95, 45%) in the blue dashed line, and the 3σ (99, 73%) in the green dashed-dotted line.

agreement; the Hubble constant is around 62 km/s/Mpc, i.e. much smaller than the one predicted by the CMB, which is around 72 km/s/Mpc, but in agreement with the ΛCDM and GCG models when only the data from SNe Ia are used; the deceleration parameter is bigger (smaller absolute value) than in those models. For the parameter estimations in the ΛCDM and in the GCG models, see Ref. [38] and references therein.

The Gaussian nature of the distribution is responsible for the fact that the best-fitting set of values is very close to the marginalized parameter estimations, with a small dispersion. Generally, this is neither true for the ΛCDM model nor for the GCG model. Again, the most remarkable differences between the viscous model and the ΛCDM model are the larger age of the Universe and the smaller absolute value of the deceleration parameter.

V. THE MATTER POWER SPECTRUM

A. The perturbed equations

In order to write the first order perturbed equations, we reexpress the field equations as

$$R_{\mu\nu} = 8\pi G\{T^v_{\mu\nu} - \tfrac{1}{2}g_{\mu\nu}T^v\} + 8\pi G\{T^b_{\mu\nu} - \tfrac{1}{2}g_{\mu\nu}T^b\}, \tag{42}$$

$$T_v^{\mu\nu}{}_{;\mu} = 0, \qquad T_v^{\mu\nu} = (\rho_v + p_v)u^\mu u^\nu - p_v g^{\mu\nu}, \tag{43}$$

$$p_v = -\xi_0 u^\mu{}_{;\mu}, \tag{44}$$

$$T_b^{\mu\nu}{}_{;\mu} = 0, \qquad T_b^{\mu\nu} = \rho_b u^\mu u^\nu. \tag{45}$$

We introduce the quantities

$$\tilde{g}_{\mu\nu} = g_{\mu\nu} + h_{\mu\nu}, \qquad \tilde{\rho} = \rho + \delta\rho, \qquad \tilde{u}^\mu = u^\mu + \delta u^\mu, \tag{46}$$

where $g_{\mu\nu}$, ρ, and u^μ are the known background solutions for the metric, the energy density, and the four velocity, respectively, and $h_{\mu\nu}$, $\delta\rho$, and δu^μ are the corresponding perturbations. We will perform the calculations using the synchronous coordinate condition

$$h_{\mu 0} = 0. \tag{47}$$

Since we will be interested mainly in perturbations that are inside the horizon, the choice of the gauge is not really essential.

The perturbed Ricci tensor takes the form

$$\delta R_{\mu\nu} = \chi^\rho_{\mu\nu;\rho} - \chi^\rho_{\mu\rho;\nu}, \tag{48}$$

where

$$\chi^\rho_{\mu\nu} = \frac{g^{\rho\sigma}}{2}[h_{\sigma\mu;\nu} + h_{\sigma\nu;\mu} - h_{\mu\nu;\sigma}], \tag{49}$$

are the perturbations of the Christoffel symbols. The relevant nonvanishing components are

$$\chi^i_{0j} = -\frac{1}{2}\left(\frac{h_{ij}}{a^2}\right)^{\cdot}, \tag{50}$$

$$\chi^0_{ij} = -\frac{\dot{h}_{ij}}{2}, \tag{51}$$

$$\chi^k_{ij} = -\frac{1}{2a^2}\{h_{ik,j} + h_{ij,k} - h_{ij,k}\}. \tag{52}$$

For the components of the perturbed energy-momentum tensor we have

$$\delta T^{00} = \delta\rho, \tag{53}$$

$$\delta T^{0i} = (\rho + p)\delta u^i, \tag{54}$$

$$\delta T^{ij} = h^{ij}p - g^{ij}\delta p. \tag{55}$$

Using the definitions

$$h = \frac{h_{kk}}{a^2}, \qquad \Theta = \delta^i_{,i}, \qquad \delta_b = \frac{\delta\rho_b}{\rho_b}, \qquad \Delta p_v = \frac{\delta p_v}{\xi_0}, \tag{56}$$

and performing a plane wave decomposition of all perturbed functions according to

$$\delta f(\vec{x}, t) = \delta f(t) e^{i\vec{k}\cdot\vec{x}}, \tag{57}$$

where $\vec{k}$ is the wave vector, we find, after a long but straightforward calculation, the following set of first order perturbed equations:

$$\ddot{h} + 2\frac{\dot{a}}{a}\dot{h} = 8\pi G(\delta\rho_v + 3\delta p_v) + 8\pi G\rho_b\delta_b, \tag{58}$$

$$\delta\dot{\rho}_v + 3\frac{\dot{a}}{a}(\delta\rho_v + \delta p_v) + (\rho_v + p_v)\left(\Theta - \frac{\dot{h}}{2}\right) = 0, \tag{59}$$

$$(\dot{\rho}_v + \dot{p}_v)\Theta + (\rho_v + p_v)\dot{\Theta} + 5\frac{\dot{a}}{a}(\rho_v + p_v)\Theta - \frac{k^2}{a^2}\delta p_v = 0, \tag{60}$$

$$\dot{\delta}_b = \frac{\dot{h}}{2}. \tag{61}$$

Replacing $\dot{h}$ by using the last relation, we obtain

$$\ddot{\delta}_b + 2\frac{\dot{a}}{a}\dot{\delta}_b - 4\pi G\rho_b\delta_b - 4\pi G\delta\rho_v - 12\pi G\xi_0\Delta p_v = 0, \tag{62}$$

$$\delta\dot{\rho}_v + 3\frac{\dot{a}}{a}(\delta\rho_v + \xi_0\Delta p_v) - (\rho_v + p_v)\Delta p_v = 0, \tag{63}$$

$$(\dot\rho_v + \dot p_v)\Theta + (\rho_v + p_v)\dot\Theta + 5\frac{\dot a}{a}(\rho_v + p_v)\Theta - \frac{k^2}{\xi_0}a^2\Delta p_v = 0, \quad (64)$$

$$\Theta - \dot\delta_b + \Delta p_v = 0. \quad (65)$$

With the help of the constraint (65), this system can be further reduced to a set of three coupled differential equations:

$$\ddot\delta_b + 2\frac{\dot a}{a}\dot\delta_b - 4\pi G\rho_b\delta_b - 4\pi G\delta\rho_v - 12\pi G\xi_0\Delta p_v = 0; \quad (66)$$

$$\delta\dot\rho_v + 3\frac{\dot a}{a}(\delta\rho_v + \xi_0\Delta p_v) - (\rho_v + p_v)\Delta p_v = 0; \quad (67)$$

$$\begin{aligned}(\dot\rho_v + \dot p_v)\dot\delta_b + (\rho_v + p_v)\ddot\delta_b + 5\frac{\dot a}{a}(\rho_v + p_v)\dot\delta_b \\ = (\dot\rho_v + \dot p_v)\Delta p_v + (\rho_v + p_v)\Delta\dot p_v + 5\frac{\dot a}{a}(\rho_v + p_v)\Delta p_v \\ + \frac{k^2}{\xi_0}a^2\Delta p_v. \quad (68)\end{aligned}$$

Now it is convenient to introduce the background equations and the quantities in Eq. (32) from which we find

$$\frac{4\pi G\rho_b}{H_0^2} = \frac{3}{2}\frac{\Omega_{b0}}{a^3}, \quad (69)$$

$$\frac{4\pi G\rho_v}{H_0^2} = \frac{3}{2}\frac{\Omega_{b0}}{a^3}[f(a)^2 - 1], \quad (70)$$

$$\frac{12\pi G\xi_0}{H_0} = \frac{1}{2}(1 - 2q_0). \quad (71)$$

The following relations will be useful later on:

$$\frac{p_v}{\rho_v} \equiv g(a) = -\frac{1}{3}\frac{f(a)}{f(a)^2 - 1}\frac{1 - 2q_0}{\sqrt{\Omega_{b0}}}a^{3/2}, \quad (72)$$

$$\dot\rho_v = -3\frac{\dot a}{a}(\rho_v + p_v), \quad (73)$$

$$\dot p_v = \frac{1 - 2q_0}{2}(\rho_v + \rho_b + p_v). \quad (74)$$

In a next step we divide the set of equations (66)–(68) by H_0^2 and redefine $H_0^{-1}\Delta p_v \rightarrow \Delta p_v$. Again, after a fairly long calculation, the perturbed equations reduce to the following system of coupled linear differential equations:

$$\ddot\delta_b + 2\frac{\dot a}{a}\dot\delta_b - \frac{3}{2}\frac{\Omega_{b0}}{a^3}\delta - \frac{3}{2}\frac{\Omega_{b0}}{a^3}(f^2 - 1)\delta_v - \frac{1}{2}(1 - 2q_0)\Delta p_v = 0, \quad (75)$$

$$\dot\delta_v - 3\frac{\dot a}{a}g\delta_v - (1 + 2g)\Delta p_v = 0, \quad (76)$$

$$\begin{aligned}(1 + g)\ddot\delta_b + \left\{2\frac{\dot a}{a}(1 + g) + \frac{1 - 2q_0}{2}\left[\frac{f^2}{f^2 - 1} + g\right]\right\}\dot\delta_b \\ = (1 + g)\Delta\dot p_v + \left\{2\frac{\dot a}{a}(1 + g) + \frac{1 - 2q_0}{2}\left[\frac{f^2}{f^2 - 1} + g\right] \right. \\ \left. + (kl_H)^2\frac{(1 - 2q_0)a}{9\Omega_{b0}(f^2 - 1)}\right\}\Delta p_v, \quad (77)\end{aligned}$$

where $l_H = c/H_0$.

Now, we reexpress the perturbed equations in terms of the variable a according to (13), which implies

$$\dot\delta = \delta'\dot a, \qquad \ddot\delta = \dot a^2\delta'' + \ddot a\delta'. \quad (78)$$

We also need the following relations, which result from the background equations:

$$\dot a^2 = \Omega_{b0}\frac{f^2}{a}, \qquad \frac{\ddot a}{\dot a^2} = -\frac{1}{2a}\left\{3g\frac{f^2 - 1}{f^2} + 1\right\}. \quad (79)$$

With the redefinition $\Delta_v = \frac{\Delta p_v}{\dot a}$, the final form for the set of perturbed equations is

$$\begin{aligned}\delta_b'' + \left\{-\frac{3}{2}g\frac{f^2 - 1}{f^2 a} + \frac{3}{2a}\right\}\delta_b' - \frac{3}{2}\frac{\delta_b}{f^2a^2} \\ = \frac{3}{2}\frac{f^2 - 1}{f^2a^2}\delta_v - \frac{3}{2}\frac{g}{a}\frac{f^2 - 1}{f^2}\Delta_v; \quad (80)\end{aligned}$$

$$\delta_v' - 3\frac{g}{a}\delta_v - (1 + 2g)\Delta_v = 0; \quad (81)$$

$$\begin{aligned}(1 + g)\delta_b'' + \left\{-\frac{3}{2}\frac{g}{a}(1 + 2g)\frac{f^2 - 1}{f^2} + \frac{3}{2a}\right\}\delta_b' \\ = (1 + g)\Delta_v' + \left\{-\frac{3}{2}\frac{g}{a}(1 + 2g)\frac{f^2 - 1}{f^2} + \frac{3}{2a} \right. \\ \left. - (kl_H)^2\frac{g}{3f^2\Omega_{b0}}\right\}\Delta_v. \quad (82)\end{aligned}$$

B. Numerical integration

Evidently, Eqs. (80)–(82) are too complicated to admit analytical solutions. Hence, we proceed integrating these equations numerically. In order to do so, an important problem is to fix the initial conditions. A scale invariant primordial spectrum (as predicted by the inflationary scenario) is assumed. But, since we are interested in the power spectrum today, we have to follow the evolution of this spectrum until the present phase.

The corresponding procedure for the ΛCDM model has been carried out in terms of the BBKS transfer function [42–44]. This function is characterized by

$$\tilde{q} = \tilde{q}(k) = \frac{k}{(h\Gamma)\ \mathrm{Mpc}^{-1}}, \qquad \Gamma = \Omega_M^0 h e^{-\Omega_B^0 - (\Omega_B^0/\Omega_M^0)}, \tag{83}$$

where Ω_M^0 and Ω_B^0 are the density parameters of dark matter and baryonic matter of the ΛCDM model. The baryonic transfer function is approximated by the numerical fit [42]:

$$T(k) = \frac{\ln(1 + 2.34\tilde{q})}{2.34\tilde{q}}[1 + 3.89\tilde{q} + (16.1\tilde{q})^2 + (5.46\tilde{q})^3 + (6.71\tilde{q})^4]^{-1/4}. \tag{84}$$

The quantity of interest is the power spectrum for the baryonic matter today. This spectrum is given by

$$P(k) = |\delta_b(k)|^2 = AkT^2(k)\frac{g^2(\Omega_T^0)}{g^2(\Omega_M^0)}, \tag{85}$$

where Ω_T^0 is the total density parameter of the ΛCDM model. The function g in (85) is the growth function

$$g(\Omega) = \frac{5\Omega}{2}\left[\Omega^{4/7} - \Omega_\Lambda + \left(1 + \frac{\Omega}{2}\right)\left(1 + \frac{\Omega_\Lambda}{70}\right)\right]^{-1} \tag{86}$$

in which Ω_Λ represents the fraction of the total energy, contributed by the cosmological constant. The normalization coefficient A in (85) can be fixed by using the cosmic background explorer (COBE) measurements of the CMB anisotropy spectrum. This coefficient is connected to the quadrupole momentum [43,44] Q_{rms} of this spectrum by the relation

$$A = (2l_H)^4 \frac{6\pi^2}{5}\frac{Q_{\mathrm{rms}}^2}{T_0^2}, \tag{87}$$

where $T_0 = 2.725 \pm 0.001$ is the present CMB temperature. The quadrupole anisotropy is taken as

$$Q_{\mathrm{rms}} = 18\mu K. \tag{88}$$

This value is obtained from the COBE normalization and is consistent with the more recent results of the WMAP measurements which use the prior of a scale invariant spectrum [44,45]. Taking all these estimates into account, one may fix

$$A = 6.8 \times 10^5 h^{-4}\ \mathrm{Mpc}^4, \tag{89}$$

which corresponds to the initial vacuum state for the density perturbations used in the BBKS transfer function.

We recall that all the relations (83)–(89) are valid for the ΛCDM model. Strictly speaking, we would have to redo all the calculations to obtain the analogue of the expression (85) for our bulk viscous model. However, since we are interested in the shape of the spectrum, there exists a simpler way which relies on the circumstance that the growth function g in (86) is a pure background quantity. Use of the ΛCDM growth function and the ΛCDM initial values also for our model will result in an overall shift of the spectrum P without affecting the structure of the latter. The resulting data will then be a fit to a "wrong," i.e. unphysical ΛCDM model, in which the composition of the dark sector differs from the standard one with roughly 30% of dark matter and 70% of a cosmological constant. However, this procedure provides us with the correct structure of the spectrum for our bulk viscous model. Keep in mind that the background dynamics of our model differs from that of the ΛCDM model by the existence of a second dark energy component (component 2) in Eq. (22).

Well inside the matter dominated phase (say, $z \sim 500$), we use the ΛCDM initial conditions, insert them in Eqs. (80)–(82), and let this system evolve. Then we compute the power spectrum $P(k) = \delta_b^2(k)$ at $z = 0$, equivalent to $a = 1$. Finally, we compare the theoretical results with the power spectrum obtained by the 2dFGRS observational program. The spectrum depends essentially on two parameters: Ω_{b0} and q_0. From now on, relying on the results

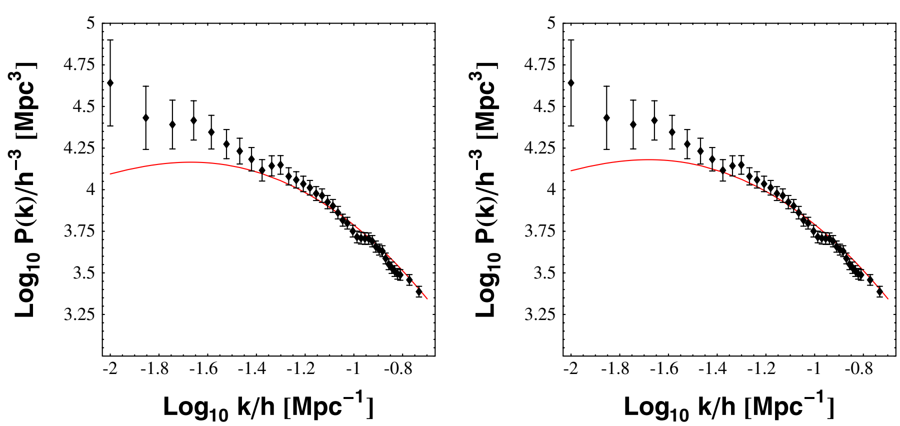

FIG. 4 (color online). Predicted power spectrum for the dark viscous fluid compared with the 2dFGRS observational data for $q_0 = -0.3$ (left) and $q_0 = -0.4$ (right). The initial conditions using the BBKS transfer function correspond to wrong ratios (see text) of dark matter and dark energy: $\Omega_{dm0} = 0.49$ and $\Omega_{\Lambda 0} = 0.51$ (left) and $\Omega_{dm0} = 0.52$ and $\Omega_{\Lambda 0} = 0.48$ (right).

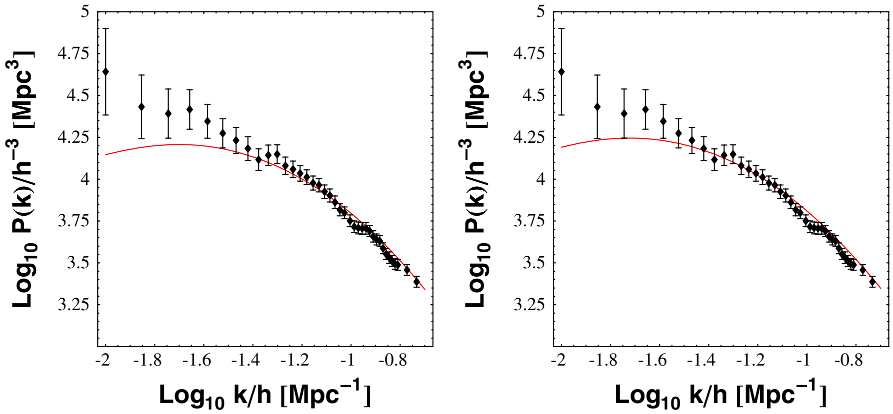

FIG. 5 (color online). Predicted power spectrum for the dark viscous fluid compared with the 2dFGRS observational data for $q_0 = -0.5$ (left) and $q_0 = -0.6$ (right). The initial conditions using the BBKS transfer function correspond to wrong ratios of dark matter and dark energy: $\Omega_{dm0} = 0.44$ and $\Omega_{\Lambda 0} = 0.56$ (left) and $\Omega_{dm0} = 0.52$ and $\Omega_{\Lambda 0} = 0.48$ (right).

of the type Ia SNe analysis and the primordial nucleosynthesis constraint, we fix $\Omega_{b0} = 0.04$ (according to the type Ia SNe analysis of the previous section, this is marginally satisfied at least at 2σ).

In Figs. 4 and 5 we present the best fitting for $q_0 = -0.3, -0.4, -0.5, -0.6$. To have a good agreement, the ratio between the quantity of dark matter/dark energy in the wrong ΛCDM reference model has to be in the range from 1 for $q_0 = -0.3$, to about $2/3$ for $q_0 = -0.6$. It is seen that the baryonic matter power spectrum of the viscous fluid model is in good agreement with the observational data for values of q_0 that are close to those predicted by the type Ia SNe analysis, that is, $q_0 \sim -0.4$. We remark *en passant* that a variation of the value of Ω_{b0} within the interval predicted by the type Ia SNe at 2σ does not change substantially the results presented in Figs. 4 and 5. In any case, there is no instability in the computed power spectrum. This is true not only for the baryonic fluid power spectrum but also for dark viscous fluid power spectrum. We note, however, that as q_0 approaches zero, there is a power depression at large scales (small k) compared with the ΛCDM reference model.

C. A physical interpretation

In the homogeneous and isotropic background, the BV model is equivalent to a GCG with $\alpha = -1/2$. The qualitative differences between both models at the perturbative level can be traced back to a difference in the pressures that characterize the cosmic medium in each of these cases. In the background both pressures coincide. But while the perturbations for the GCG are entirely adiabatic, this is not the case for our present model.

In the background we have $p = p_v = -3H\xi_0$ for the viscous fluid and $p = -E\rho^{1/2}$ for the GCG with $\alpha = -1/2$ (cf. (19)). Use of Friedmann's equation $3H^2 = 8\pi G\rho$ (for the spatially flat case) reveals that in both cases we have an equation of state $p \propto -\rho^{1/2}$, where the constants are related by $E = \xi_0\sqrt{24\pi G}$. The first order pressure perturbations for the GCG are

$$\delta p = \frac{\dot{p}}{\dot{\rho}}\delta\rho \qquad \text{(GCG model)}, \tag{90}$$

where

$$\frac{\dot{p}}{\dot{\rho}} = -\alpha\frac{p}{\rho} \qquad \text{(GCG model)} \tag{91}$$

is the adiabatic sound speed square. For $\alpha > 0$ the sound speed square is positive, giving rise to a (nonobserved) oscillatory behavior. For $\alpha < 0$ (our case) this square is negative which results in instabilities which are not observed either.

For the viscous fluid the pressure perturbations are qualitatively different. In particular, the propagation of perturbations is no longer given by the adiabatic sound speed. The perturbations are nonadiabatic. The nonadiabaticity is characterized by

$$\delta p - \frac{\dot{p}}{\dot{\rho}}\delta\rho = -\dot{p}\left(\frac{\delta\rho}{\dot{\rho}} - \frac{\delta H}{\dot{H}}\right) \qquad \text{(BV model)}, \tag{92}$$

where $\delta H \equiv \delta(u^{\mu}_{;\mu})/3$. In general, the right-hand side of (92) does not vanish (for a similar situation see [46]). It is this nonadiabatic character of the perturbations which makes the power spectrum well behaved on small scales in contrast to the GCG case. A more detailed analysis of this feature will be given elsewhere.

VI. CONCLUSIONS

We presented a two-component cosmological model in which one component represents the dark sector, the other one pressureless baryons. The dark sector is described by a single bulk viscous fluid with a constant bulk viscosity coefficient $\xi = \xi_0 =$ constant. A dynamical system analysis was used to show that the assumption of a constant ξ does not seem to be too restrictive and that this model embodies quite general features and does not represent a very particular configuration. In the homogeneous and isotropic background the total energy density (i.e., including the baryons) is equivalent to that of a GCG with $\alpha = -1/2$. But while the perturbation dynamics of a GCG is entirely adiabatic, the present model exhibits nonadiabatic features. As a consequence, it can avoid the problems that usually plague such type of unified dark matter/dark energy models, namely, the appearance of (nonobserved) small scale oscillations or instabilities. The predictions of our model were compared with SNe Ia data and with the 2dFGRS results. For the comparison with SNe Ia data we employed the so-called gold sample of 182 good quality high redshift supernovae. Our Bayesian statistics analysis leads to the following parameter evaluation at 2σ level: $q_0 = -0.357^{+0.130}_{-0.123}$, $\Omega_{b0} = 0.055^{+0.011}_{-0.011}$, $H_0 = 62.34^{+1.75}_{-1.72}$ km/s/Mpc, and $t_0 = 15.85^{+0.91}_{-1.08}$ Gy. The main differences in comparison with a similar analysis for the ΛCDM and the GCG models [38] are: the age of the Universe is considerably larger; the deceleration parameter is larger (smaller in absolute value); the baryon density is only marginally compatible with the primordial nucleosynthesis result. A remarkable feature is the (almost) perfect Gaussian distribution for all parameters with a quite small dispersion.

To compare the results of our perturbation analysis with the observed matter power spectrum we have used the BBKS transfer function to fix the initial condition at a very high redshift ($z \sim 500$), deep in the matter dominated phase. Since the BBKS transfer function has been conceived for a two-component description of the dark sector, dark matter, and a cosmological constant, this must be seen with some caution. We have argued that, in spite of this problem, the resulting power spectrum preserves its shape and can be compared with observations. A good fitting can be obtained for values of q_0 which are in agreement with the type Ia SNe analysis. The best results are found for $-0.3 \gtrsim q_0 \gtrsim -0.6$. Qualitatively, our analysis confirms previous results for a simplified model of the cosmic medium, in which the baryon component was neglected [28].

ACKNOWLEDGMENTS

J. C. F. thanks the IMSP (Benin) for the warm hospitality during part of the elaboration of this work. He thanks also CNPq (Brazil) and the CAPES/COFECUB French-Brazilian scientific cooperation for partial financial support. W. Z. acknowledges support by grants No. 308837/2005-3 (CNPq) and No. 093/2007 (CNPq and FAPES).

[1] A. G. Riess *et al.*, Astron. J. **116**, 1009 (1998); S. Perlmutter *et al.*, Astrophys. J. **517**, 565 (1999).
[2] J. L. Tonry *et al.*, Astrophys. J. **594**, 1 (2003).
[3] A. G. Riess, Astrophys. J. **607**, 665 (2004).
[4] P. Astier *et al.*, Astron. Astrophys. **447**, 31 (2006).
[5] D. N. Spergel *et al.*, Astrophys. J. Suppl. Ser. **170**, 377 (2007).
[6] M. Tegmark *et al.*, Phys. Rev. D **69**, 103501 (2004).
[7] S. W. Allen, R. W. Schimdt, H. Ebeling, A. C. Fabian, and L. van Speybroeck, Mon. Not. R. Astron. Soc. **353**, 457 (2004).
[8] E. V. Linder, J. Cosmol. Astropart. Phys. 04 (2007) 004.
[9] A. Lewis and A. Challinor, Phys. Rep. **429**, 1 (2006).
[10] S. Hannestad, Int. J. Mod. Phys. A **21**, 1938 (2006).
[11] A. Yu. Kamenshchik, U. Moschella, and V. Pasquier, Phys. Lett. B **511**, 265 (2001).
[12] J. C. Fabris, S. V. B. Gonçalves, and P. E. de Souza, Gen. Relativ. Gravit. **34**, 53 (2002).
[13] M. C. Bento, O. Bertolami, and A. A. Sen, Phys. Rev. D **66**, 043507 (2002).
[14] H. Sandvik, M. Tegmark, M. Zaldarriaga, and I. Waga, Phys. Rev. D **69**, 123524 (2004).
[15] J. C. Fabris and H. Velten (work in progress).
[16] A. B. Balakin, D. Pavón, D. J. Schwarz, and W. Zimdahl, New J. Phys. **5**, 85 (2003).
[17] R. R. R. Reis, I. Waga, M. O. Calvão, and S. E. Joràs, Phys. Rev. D **68**, 061302 (2003).
[18] W. Zimdahl and J. C. Fabris, Classical Quantum Gravity **22**, 4311 (2005).
[19] V. A. Belinskii and I. M. Khalatnikov, Sov. Phys. JETP **42**, 205 (1975).
[20] J. D. Barrow, Phys. Lett. B **180**, 335 (1986); Nucl. Phys. **B310**, 743 (1988); *The Formation and Evolution of Cosmic String*, edited by G. W. Gibbons, S. W. Hawking, and T. Vachaspati (Cambridge University Press, Cambridge, England, 1990), p. 449.
[21] R. Maartens, Classical Quantum Gravity **12**, 1455 (1995).
[22] W. Zimdahl, Phys. Rev. D **53**, 5483 (1996).
[23] R. Maartens, in *Proceedings of the Hanno Rund Conference on Relativity and Thermodynamics*, edited by S. D. Maharaj (University of Natal, Durban, 1997), p. 10.
[24] W. Zimdahl, Phys. Rev. D **61**, 083511 (2000).
[25] W. Zimdahl, D. J. Schwarz, A. B. Balakin, and D. Pavón, Phys. Rev. D **64**, 063501 (2001).
[26] T. Padmanabhan and S. M. Chitre, Phys. Lett. A **120**, 433 (1987).
[27] M. Szydłowski and O. Hrycyna, arXiv:astro-ph/0602118.
[28] J. C. Fabris, S. V. B. Gonçalves, and R. de Sá Ribeiro, Gen. Relativ. Gravit. **38**, 495 (2006).
[29] C. Eckart, Phys. Rev. **58**, 919 (1940).
[30] W. Israel and J. M. Stewart, Proc. R. Soc. A **365**, 43 (1979).

[31] W. Israel and J. M. Stewart, Ann. Phys. (N.Y.) **118**, 341 (1979).
[32] Jian-Huang She, J. Cosmol. Astropart. Phys. 02 (2007) 021.
[33] A. A. Coley and R. J. van den Hoogen, Classical Quantum Gravity **12**, 1977 (1995).
[34] J. G. Bartlett and J. Silk, Astrophys. J. **423**, 12 (1994); J. G. Bartlett, Astrophys. Space Sci. **290**, 105 (2004).
[35] M. C. Bento, O. Bertolami, and A. A. Sen, Phys. Rev. D **70**, 083519 (2004).
[36] G. Sansone and R. Conti, *Equazioni Differenziali Non Lineari* (Edizioni Cremonense, Roma, 1956).
[37] A. G. Riess *et al.*, arXiv:astro-ph/0611572.
[38] R. Colistete, Jr., J. C. Fabris, S. V. B. Gonçalves, and P. E. de Souza, Int. J. Mod. Phys. D **13**, 669 (2004); R. Colistete, Jr., J. C. Fabris, and S. V. B. Gonçalves, Int. J. Mod. Phys. D **14**, 775 (2005); R. Colistete, Jr. and J. C. Fabris, Classical Quantum Gravity **22**, 2813 (2005); R. Colistete, Jr. and R. Giostri, arXiv:astro-ph/0610916.
[39] S. Weinberg, *Gravitation and Cosmology* (Wiley, New York, 1972).
[40] P. Coles and F. Lucchin, *Cosmology* (Wiley, New York 1995).
[41] W. Freedman, Astrophys. J. **553**, 47 (2001).
[42] J. M. Bardeen, J. R. Bond, N. Kaiser, and A. S. Szalay, Astrophys. J. **304**, 15 (1986).
[43] N. Sugiyama, Astrophys. J. Suppl. Ser. **100**, 281 (1995).
[44] J. Martin, A. Riazuelo, and M. Sakellariadou, Phys. Rev. D **61**, 083518 (2000).
[45] G. Hinshaw *et al.*, Astrophys. J. Suppl. Ser. **170**, 288 (2007).
[46] W. Zimdahl, arXiv:0705.2131v1.